*

Hydrological characterization of acidic pit lakes in the Tharsis mines (Iberian Pyrite Belt): the evolution of flood levels and future trends.

Raúl Moreno González[a,b], Manuel Olías[a,b], Francisco Macías[a,b], Carlos Ruiz Cánovas[a,b]*, Rubén Fernández de Villarán[c],

[a] Department of Earth Sciences, Faculty of Experimental Sciences, University of Huelva, Campus 'El Carmen' s/n, 21071 Huelva, Spain

[b] Research Center on Natural Resources, Health and the Environment (RENSMA), University of Huelva, 21071 Huelva, Spain

[c] Department of Agroforestry Sciences, University of Huelva, Campus 'La Rábida', 10 21071-Palos de la Frontera, Huelva, Spain.

* Corresponding author: Carlos Ruiz Cánovas (carlos.ruiz@dgeo.uhu.es), phone +34 959219870, ORCID number 0000-0002-2860-5154

Abstract

Opencast mining operations frequently lead to the creation of large voids that become anthropogenic lakes when the water table recovers. In the case of coal, and especially sulfide mining, the stored water is of an acidic nature with significant concentrations of toxic metals and, therefore, a high pollutant potential. The present work analyzes the status of four acidic mine pit lakes in the Tharsis mines, which is the second most important mine district in the Iberian Pyrite Belt (IPB), after the Río Tinto mines. The accumulation of huge volumes of acidic and metal-rich waters (5.2 Mm^3) in these pit lakes poses a serious environmental concern; approximately 9,000 tons of Fe, 1,000

tons of Al and Zn, and large amounts of other toxic metals are currently stored in the pit lakes. The water level in Sierra Bullones and Filón Norte, the largest lakes, shows an average rise of approximately 2.8 m/yr, which would lead to an overflow by 2051 if the trend continues. However, the increase in the evaporation rate that is expected as a result of the larger surface area during flooding episodes would induce a hydrological equilibrium before reaching the overflow level, leading to the formation of a terminal lake. On the other hand, the water level in Filón Centro and Filón Sur Pit Lakes remain approximately stable. The methodology used in the present work may be of interest to be applied in abandoned opencast mining areas in other regions worldwide.

Keywords; flooding prediction; acid mine drainage; metal pollution; water management; water balance.

1. INTRODUCTION

Mine closure constitutes one of the biggest environmental problems worldwide (Younger et al. 2002; Sarmiento et al. 2009; Robles-Arenas and Candela 2010). In surface mining, large open pits are created. The cease of pumping once mining activities end generally leads to the progressive flooding of the open pits, generating pit lakes. The hydrological equilibrium of the pit lake is achieved when water inputs are equal to losses by evaporation or when overflows are produced on the surface and in subterranean areas, generating a discharge of polluted water to rivers or aquifers. The release of these waters can pose substantial environmental concerns (Davis and Ashenberg 1989; Savage et al. 2000; Castendyk 2011; Castendyk et al. 2015a, 2015b; Boehrer et al. 2016). For example, in May 2017, the breakage of a mine gallery led to

48 the spill of around 300,000 m^3 of acidic waters from the La Zarza pit lake (southwestern
49 Spain), causing a sharp impact on the Odiel River, which resulted in the adoption of
50 urgent restoration measures.

51 In the case of sulfide mining, the problem is worse because pit lakes usually store acidic
52 waters with extreme concentrations of toxic metals (Sánchez España et al. 2008;
53 Cánovas et al. 2015) that are of a high pollutant potential (Nordstrom et al. 2015). This
54 is also frequently observed in coal mining, although the acidity input into the lakes is
55 not usually as high as in sulfide mine pit lakes. The water quality of the pit lake depends
56 on the balance between the acidity and alkalinity inputs into the lake together with the
57 neutralization processes in the water column (Blodau 2006; Castendyk et al. 2015b).
58 There are currently several models that use information from these processes to predict
59 the final water quality after mining cessation (Oldham et al. 2009; Vandenberg et al.
60 2011; Geller et al. 2013; Castendyk et al. 2015b). However, the first step to
61 implementing these models would be to acquire a detailed knowledge of the
62 hydrological dynamics of pit lakes and their surroundings.

63 The Iberian Pyrite Belt (IPB) is one of the biggest polymetallic sulfide deposits in the
64 world, and it constitutes a huge environmental concern due to the large volume of acidic
65 waters stored in pit lakes. The intense mining activity mainly developed during the
66 second half of the nineteenth and early twentieth centuries has left an impressive
67 environmental legacy, with huge amounts of widespread mine wastes close to the mine
68 sites, which have and important impact on the Tinto and Odiel Rivers (see, for example,
69 Sánchez España et al. 2005; Cánovas et al. 2016; Olías et al. 2016). As a consequence
70 of the ceased mining at the end of the twentieth century, there are 22 flooded open pits
71 in the Spanish part of the IPB (Sánchez España et al. 2008). Most of these pit lakes
72 contain acidic water and lack management or control plans. Although the

hydrogeochemical and limnological properties of some of these pit lakes have been previously studied (see, for example, Sanchez España et al. 2008; Santofimia and López-Pamo 2013; Cánovas et al. 2015), some of them have not achieved equilibrium, and their hydrological connection of the IPB acidic pit lakes with the surrounding mines and aquifers is not well understood (Sánchez-España et al. 2014). This information is of paramount importance to foresee their evolution, to plan potential remediation measures, and to avoid potential environmental risks.

This issue is especially relevant for the Tharsis mine complex, which constitutes one of the most important exploitations of the IPB. This derelict district hosts five open pits, four of which are partially flooded by acidic and extremely metal-rich waters (Sánchez España et al. 2008). In addition, there is a surface of around 3.6 km^2 covered by mine waste that generate acidic leachates. As a consequence, main water bodies in the drainage basin are deeply polluted. Some of the acidic leachates generated in the Tharsis mine complex join the Meca River, which feeds the Sancho Reservoir (58 Mm^3). The Sancho Reservoir has suffered a progressive acidification in recent years, and it is considered to be one of the more extreme cases of surface water pollution worldwide (Cánovas et al. 2016). A large reservoir (246 Mm^3) is currently under construction to receive the acidic leachates from the Tharsis mine complex (Olías et al. 2011). If additional leachates were generated from existing pit lakes, the water quality of local streams and reservoirs would worsen.

Based on the concerns described above, the main goals of the present work are: 1) to analyze the flooding evolution of the pit lakes of the Tharsis mine complex; 2) to obtain a conceptual model of the hydrological behavior of the pit lakes and perform a water balance of each system and; 3) to predict the evolution of these pit lakes in the long

97 term. This information is critical to identifying and adopting cost-effective measures to
98 mitigate the impact of acidic waters in local receiving water bodies.

99

100 ## 2. SITE DESCRIPTION

101 The Tharsis mining complex has a Mediterranean climate with an average yearly
102 precipitation close to 600 mm, but it exhibits high intra- and inter-annual variability
103 (Galván et al. 2009). Average temperatures in the area are close to 16.5ºC. Summers are
104 hot and dry, with maximum temperatures close to 40ºC, while winters are humid and
105 cold (minimum temperatures lower than 0ºC). The most important water courses are the
106 Aguas Agrias Creek, which joins the Oraque River (feeding the Alcolea projected
107 reservoir) to the east, and the Meca River, which is located in the south and is regulated
108 by the Sancho Reservoir (Fig. 1).

109 Original sulfide reserves in the Tharsis mine complex are estimated to be around 133
110 Mt (Tornos et al. 2009). Sulfide mining in Tharsis, like many other mines in the IPB,
111 started around 5,000 years ago during the Chalcolithic period (Nocete et al. 2005). After
112 a period of inactivity, mining restarted during the Tartessian and Roman periods
113 (Gonzalo y Tarín 1888). Afterwards, a long period of low mining activity continued
114 until 1856 when the mine was rediscovered (Deligny 1863) and underground mining
115 was performed, mainly by room and pillars in Filón Norte, Sierra Bullones, Filón
116 Centro, and Filón Sur (Fig. 1). Opencast mining started in 1866 in Filón Norte, and
117 some years later in Sierra Bullones and Filón Centro (Gonzalo y Tarín 1888). Mining in
118 Filón Centro and Filón Norte ceased in 1884 and 1890, respectively, and focused on
119 mineral exploitation in Sierra Bullones by both opencast and underground mining.

Since the beginning of the twentieth century, sulfur from pyrite was obtained to produce sulfuric acid. However, a new processing method was developed in Filón Sur from 1937 to 1964 to extract Au and Ag from the gossan (Checkland, 1967). In the mid-twentieth century, mining was restarted in Filón Centro, leading to an increase in the open pit. Around 1960, a new period of exploitation in the Filón Norte open pit also began. Mining ceased in Sierra Bullones in 1966 (after 100 years of intense exploitation), while Filón Norte mining finished at the end of the 90s. The last mining activities developed in the Tharsis mine complex were performed in Filón Sur from 1990 to 2001 to obtain Au and Ag by cyanide leaching of the gossan.

From 1856 to 2001, approximately 40 Mt of sulfide were obtained (Tornos et al. 2009). Approximately 17 Mt were obtained up to 1960, mainly from Sierra Bullones (Pinedo Vara 1963), while the rest were obtained mainly from Filón Norte during the last 40 years of exploitation. About 5 Mt of mineral must be added to these figures from mining developed during the Roman and pre-Roman periods (Gonzalo y Tarín 1888).

3. METHODOLOGY

3.1.Water level and total volume stored in the pit lakes

In order to estimate the flooding evolution of the pit lakes, digital terrain models (DTM) for 1998 (with a horizontal resolution of 20 x 20 m) and 2001–2002 (with a horizontal resolution of 10 x 10 m) was used, together with available orthophotographs (July 1998, October 2002, August 2004, October 2005, May 2007, May 2009, August 2011, May 2013, and July 2016). Aerial photographs prior to these periods were also looked at to check the flooding status of the pit lakes. An online mapping tool called ArcGis was

144 used to estimate the water level and the volume of stored water in the pit lakes. Due to
145 the absence of water-level records, the following methodology was applied: 1) the
146 flooded surface was estimated from orthophotographs for each pit lake; 2) the
147 relationship between the altitude and pit surface was estimated by DTM, which allowed
148 the water level to be established from the flooded surface; and 3) the volume of stored
149 water was calculated from the water level and the DTM using the ArcGis Surface
150 Volume tool.

151

152 **3.2.Water balance in the pit lakes**

153 Daily precipitation was obtained from a rainfall gauge located close to the studied pit
154 lakes (Fig. 1). Evaporation was calculated from the equation of Penman (1948):

$$EV = \frac{\Delta Rad_n + \gamma E_a}{\Delta + \gamma} \quad (1),$$

155 where EV is evaporation from a free surface (mm/day), Δ is the slope of the saturation
156 vapor pressure curve (kPa/ºC), γ is the psychrometric constant (kPa/ºC), Rad_n is the net
157 irradiance (mm/day), and E_a is the heat capacity of air (mm/day). The detailed
158 estimation procedure is described by Allen et al. (1998). The information required to
159 apply Equation 1 (that is, the latitude; height above sea level; and daily data for
160 maximum and minimum temperatures, maximum and minimum values of relative
161 humidity, wind speed, and solar radiation) were obtained from a meteorological station
162 located 12 km to the west of the Tharsis mine complex.

163 The water balance in the pit lakes was estimated from rainfall data, runoff data,
164 evaporation data, and the difference in volume observed between orthophotographs.
165 Water inputs to the pit lakes were estimated by considering the runoff generated in the

drainage basin and the direct precipitation on the pit lake surface. This latter value was obtained by multiplying the rainfall collected between consecutive orthophotographs by the average flooded surface at the beginning and the end of the period, as follows:

$$DR_n = R_n \times \frac{Af_n - Af_{n-1}}{2} \quad (2),$$

where DR_n are the water inputs by direct rainfall during the period n (m^3), R_n is the precipitation during the period n (m), and Af_n and Af_{n-1} are the flooded surfaces during the period n and n-1 (m^2).

The runoff generated was obtained by multiplying the precipitation collected between the times of the consecutive orthophotographs by the total surface of the drainage basin. The runoff coefficient (C) was obtained for the selected area by the SWAT hydrological model (Galván et al., 2009):

$$Qrun_n = R_n \times (A_{catch} - \frac{Af_n - Af_{n-1}}{2}) \times C \quad (3),$$

where $Qrun_n$ and R_n are the runoff and precipitation amounts during the period n, A_{catch} is the drainage basin of each pit lake, and Af_n and Af_{n-1} are the flooded surfaces during periods n and n-1, respectively.

The sum of Equations 2 and 3 correspond to the surface water input to each pit lake (I_n, Eq. 4):

$$I_n = Qrun_n + DR_n \quad (4),$$

In order to estimate the water losses, the amount of evaporation estimated in Equation 1 was multiplied by the average flooded surface of each pit lake at the beginning (Af_{n-1}) and the end of the period (Af_n):

$$O_n = Ev_n \times \frac{Af_n - Af_{n-1}}{2} \quad (5),$$

where O_n is the volume of water lost by evaporation during the period n (m^3), and Ev_n is the evaporation during the period n (m).

In addition, groundwater inputs were estimated for each period as the difference between inputs (I_n), losses (O_n), and the variation of water stored in the pit lake:

$$Qsub_n = (I_n - O_n) - (V_n - V_{n-1}) \quad (6),$$

where $Qsub_n$ are groundwater inputs during the period n, and V_n and V_{n-1} are the volumes of water stored during the periods n and n-1, respectively.

3.3. Estimation of pollutants contained in pit lakes

Samples of surface water from the pit lakes were taken in 2016, with the exception of Sierra Bullones, which was not accessible. Samples were collected in high-density polyethylene (HDPE) bottles that were previously washed with a solution of 10% HNO_3, filtered through 0.45 μm, and acidified to pH < 2. Temperature, pH, electrical conductivity (EC), and oxidation-reduction potential (ORP) were measured in situ using a Crison MM40+ multimeter. A three-point calibration was performed for both EC (147 μS/cm, 1,413 μS/cm, and 12.88 mS/cm) and pH (4.01, 7.00, and 9.21), while ORP was controlled using two points (240 and 470 mV). Net acidity was also calculated according to Kirby and Cravotta (2005), considering both the free acidity and that generated by hydrolysable metals: Fe, Al, Mn, Cu, or Zn. Samples were analyzed at the R+D laboratories of at the University of Huelva by 1) Inductively Coupled Plasma-Atomic Emission Spectroscopy for Al, Cu, Fe, Mn, S, and Zn, determination and by 2)

206 Inductively Coupled Plasma-Mass Spectroscopy (ICP-MS) for As, Cd, Co, Cr, Ni, and
207 Pb. Detection limits were 200 µg/L for Al, Fe, Mn, and S; 50 µg/L for Zn; 5 µg/L for
208 Cu; and 0.1 µg/L for As, Cd, Co, Cr, Ni, and Pb.

209 The estimations of the acidity, sulfates, and metal and metaloids stored in the pit lakes
210 were performed by multiplying the volume of water of each pit lake (section 3.1) by the
211 corresponding concentration. This estimation can be considered only as an approach due
212 to concentration variations within the water column were not considered.

213

214 **4. RESULTS AND DISCUSSION**

215

216 **4.1.Rainfall and evaporation evolution**

217 Figure 2 shows the annual evolution of precipitation and evaporation from 1998 to
218 2016. Rainfall distribution exhibited was highly variable, with values ranging from 261
219 to 1,009 mm/yr, and a mean of 662 mm/yr. The driest years were 1998–1999, 2004–
220 2005, and 2011–2012, while the rainiest were 2000–2001, 2009–2010, and 2010–2011.
221 Notably, values of evaporation exceed those of precipitation (average value of 1,699
222 mm/yr), in turn, showing a lower variability, with values ranging from 1,530 (2013–
223 2014) to 1,938 mm (2002–03).

224

225 **4.2.Current status of the pit lakes**

226 Except Esperanza pit, which is partially filled with mine wastes and open to the east, all
227 of the open pits are currently flooded. The deepest and largest pit is, by far, Filón Norte,
228 with a total surface area of 0.52 km^2 (Table 1), and the pit with the largest drainage

basin is Sierra Bullones (1.04 km^2). Filón Centro and Filón Sur have achieved a hydrological equilibrium. In the case of Filón Centro, the pit has been flooded since at least 1977 (which is the first aerial photograph where the occurrence of water is appreciated). Filón Sur was dry in 1998, while the flooding is evident from 2002. Nevertheless, small fluctuations are observed depending on the month of the year when the orthophotograph was acquired, with higher values during the rainy season and lower values during the dry season (the water level in Filón Sur ranges from 255.7 to 257.0 m and in Filón Centro from 258.2 to 258.7 m). On the contrary, the flooding of Filón Norte and Sierra Bullones remains active, so the occurrence of overflow into the surrounding water courses in the future is expected.

There were 5.2 Mm^3 of acid mine drainage (AMD) in the different pit lakes in June 2016 (Table 2), most of which were in Filón Norte (3.58 Mm^3). The stored waters are characterized by having a high acidity (pH of 2.2–2.3 and a net acidity of 3.6–7.1 g $CaCO_3$/L) and concentration of metals and metaloids (for example, up to 2,053 mg/L of Fe, 228 mg/L of Zn, and 11 mg/L of As). The most polluted water was that of Filón Norte (Table 2). Comparing the samplings carried out between 2005 and 2006 by Sanchez España et al. (2008), the concentrations obtained from Filón Centro in this study were similar, but the concentrations obtained from Filón Sur and Filón Norte have diminished substantially (for example, Fe has decreased from 1,922 to 774 mg/L in Filón Sur and from 4,620 to 2,053 in Filón Norte). This decrease is likely related to the fact that Filón Centro is a mature open pit, while the other two have not yet reached stable conditions.

The stored mass of pollutant has been calculated from the volumes and the analyzed concentrations. Since Sierra Bullones and Filón Norte are connected underground, it has been suggested that concentrations in Sierra Bullones are the same as that in Filón

Norte. The total acidity and metal and metaloid load stored in the pit lakes is remarkable, for example, approximately 32,000 ton of $CaCO_3$, 10,000 ton of Fe, 1,000 ton of Al and Zn, and 46 ton of As (Table 2). The impact of a potential release of these waters to receiving water bodies can be appreciated when comparing these results with the annual load carried out by the Meca River (Galván et al. 2012); the amount of dissolved Fe stored in the pit lakes is around 35 times higher than that annually carried by this river.

4.3. Flooding evolution in Filón Norte and Sierra Bullones

Figure 3 shows the orthophotographs of Filón Norte and Sierra Bullones from 1998 to 2016. It can be noted that flooding had not started in both pits in 1998; however, flooding in Filón Norte was evident in 2002, while flooding in Sierra Bullones was noticeable in 2004 (this orthophotograph is not shown in Fig. 3). Since then, the water level has risen in both pit lakes, increasing the flooded surface and, therefore, the volume of AMD stored.

The water level in both pit lakes has been estimated from the DTM and the orthophotographs. The evolution of the water level is quite similar in both pit lakes, although slightly higher values are observed in Sierra Bullones. This similar behavior is due to both pit lakes may be hydrologically connected by underground galleries. The water level in Filón Norte has risen around 40 m from 2002 to 2016, which accounts for an average rise of 2.8 m/yr. It can be also noted that the water level rise was sharper during the first few years, and it then seems to have plateaued since that time, following a second- order polynomial regression (Fig. 4A). However, the change in water level is influenced by rainfall distribution, with such as wet periods where during which the

278 water level rise is higher (for example, between November -2002 to August- 2004) and
279 dry ones years during which the rise is lower than expected according to the general
280 tendency (for example, June 2007 to May 2009). The volume of stored water shows a
281 tendency that is approximately lineal over the time (Fig. 4B), although with some
282 deviations due to the rainfall distribution, as previously discussed.

283

284 **4.4. Water balance and hydrological dynamics of the pit lakes**

285 *4.4.1. Filón Centro*

286 Table 3 shows the water inputs and losses in Filón Centro. The flooded surface area
287 remained approximately constant during the study period (approximately 3.6 hm^2), with
288 the exception of hydrological year of 2004–2005, which showed a clearly lower surface
289 area due to the orthophotograph coinciding with the lowest value of precipitation (Fig.
290 2). The volume of AMD stored in the pit lake was around 1.1 Mm^3. Runoff accounted
291 for more than half of the water inputs into the pit lake, whereas the rest corresponded to
292 direct precipitation. Generally, the water losses were slightly higher than inputs, which
293 means Filón Centro may receive hidden inputs from the waste dumps located to the
294 west and from groundwater (Fig. 5). However, water inputs were higher than losses
295 during the rainy periods (from November 2005 to May 2007 and from June 2009 to
296 August 2011; Table 3). A permanent acidic outflow was identified that arose from the
297 bottom of a waste dump located to the west of Filón Centro, and the flow was generally
298 between 0.1 and 0.5 L/s. This outflow was found at a lower level (240 m) than the water
299 level in the pit lake (258 m); thus, water losses may occur at this point during rainy
300 periods (Fig. 5A). Therefore, Filón Centro would behave as a terminal lake during dry
301 seasons (Castendyk 2011; Castendyk et al. 2015a), and the rise above a certain level as

a consequence of rainfalls would cause the pit lake to behave as a flow-through pit lake (Fig. 5B), releasing water through the waste dump to the west.

4.4.2. Filón Sur

The drainage basin of Filón Sur as recorded during the study was relatively large (29 hm^2; Table 1), while the flooded surface area (0.6 hm^2) and the volume of stored AMD (6,000 m^3) were small. Thus, the surface water inputs to the lake were mainly due to runoff (Table 3, Fig. 6). Water losses by evaporation were noticeably lower than surface inputs. As the water level was approximately constant (see section 4.2), this pit lake must have hidden water losses. These losses were thought to occur through La Sabina underground gallery located to the south (Fig.1). However, the water level in the pit lake (257 m) is clearly higher than the altitude of La Sabina adit (Fig. 6). In addition, monitoring in La Sabina from the end of 2015 showed evidence of a low average discharge (0.6 L/s; Olías et al. 2017) without significant changes in response to rainfalls, which is inconsistent with a possible overflow from Filón Sur (Fig. 6).

Water exits from Filón Sur probably occur through an unnoticed derelict gallery constructed to the east at the end of the nineteenth century (Gonzalo y Tarín 1888). This adit can be seen at the surface of the pit lake, although the exit toward Corta Esperanza is not visible and is likely buried by mine wastes (Fig. 6). On the other hand, Cánovas et al. (2017) reported that the acidic outflows from the Corta Esperanza area to be the main AMD contributor to the Meca River and the Sancho Reservoir (Fig. 1) with a quick response to rainfalls, which could be related to water exits from Filón Sur.

4.4.3. Sierra Bullones and Filón Norte

The drainage basin of Sierra Bullones is the largest of the whole pit lakes (104 hm^2; Table 1); the runoff generated after rainfalls accounts for around 95% of water inputs to

326 the pit lake (Table 3). Surface water inputs are considerably higher than losses by
327 evaporation due to the small flooded surface area, although the latter increases
328 progressively (Table 3). The difference between water inputs and losses estimated for
329 each period assessed was much higher than the increase of water stored in the pit lake.
330 Therefore, undetected water losses may occur from this pit lake to Filón Norte through
331 underground galleries (Fig. 7). Thus, Sierra Bullones also behaves as a flow-through pit
332 lake.

333 Runoff constitutes the main contributor to Filón Norte pit lake, with a drainage basin of
334 60 hm^2; however, as long as the flooded surface increases, the percentage of direct
335 precipitation rises (Table 3). Losses by evaporation step up progressively and are linked
336 to the increase in the flooded surface area, although some decreases in evaporation can
337 be seen on Table 3 because the periods are shorter (September 2004 to October 2005) or
338 have a higher proportion of winter days (September 2011 to May 2013). Thus, losses by
339 evaporation are generally lower than surface water inputs during the first flooding stage,
340 while the situation reverses in the last periods. Nevertheless, as commented before,
341 Filón Norte must receive unnoticed outflows from Sierra Bullones.

342 Groundwater inputs to Sierra Bullones and Filón Norte have been estimated from
343 Equation 6. These inputs have negative values in Sierra Bullones, which is evidence of
344 the existence of groundwater outputs (Fig. 8). During the first stages of flooding (until
345 May 2009), water inputs to Filón Norte coincide approximately with losses from Sierra
346 Bullones due to the hydrological connection between both pit lakes. Groundwater inputs
347 to both pit lakes—that is, the difference between inputs to Filón Norte and losses to
348 Sierra Bullones—are low. However, water inputs to Filón Norte were higher than losses
349 from Sierra Bullones since 2011, which is evidence of an increase in groundwater flows
350 to the pit lakes. This water level rise in the pit lake may cause a decrease in the

hydraulic gradient and, thus, a corresponding increase in the groundwater inputs to the lakes (Marinelli and Niccoli 2000). This could be explained by the fill of unknown mining voids. Groundwater inputs during the first stages of flooding may cause an inundation of these voids, resulting in less water entering into the pit lakes.

As can be seen in Figure 4, the water level in Filón Norte and Sierra Bullones has been rising progressively. The outflow level in Filón Norte is found to the east of the pit lake at 235 m, where a derelict mine tunnel to transport minerals is located (Fig. 7). The maximum water level in Sierra Bullones is expected to be the same as in Filón Norte due to both pit lakes being connected underground. According to the polynomial equation for the evolution of the water level at Filón Norte (Fig. 4A), the overflow would be reached by 2051.

However, the water level rise is causing incremental losses by evaporation and a decrease in the hydraulic gradient toward the pit lake. A hydrogeological model would be needed to reliably predict the flooding evolution of the pit lake, which requires detailed information, such as piezometric levels, radius of influence, and horizontal hydraulic conductivity (Marinelli and Niccoli 2000). In addition, high-resolution measures of these parameters should be obtained due to the high heterogeneity and geological complexity of the area. As this information is not available, a simple approach for estimating the evolution of the water level has been followed. For the open pits of both Filón Norte and Sierra Bullones, it has been assumed that the groundwater inputs are similar to those obtained in section 4.4.3 for the most recent period (2013–2016). Thus, considering average values of annual precipitation and evaporation (mm/yr), it can be estimated that the evaporation of the water surface is necessary to balance the inputs. If the equilibrium water surface for both open pits is 34.7 hm^2, corresponding to a water level of 228.5 m, which is below the water outflow level (235

376 m), both open pits would behave as a terminal lakes. This calculation must be
377 considered as an approach to predict the flooding evolution of these pit lakes, and a
378 monitoring of water levels should be carried out in the future.

379

380 **CONCLUSIONS**

381 The mining activities in Tharsis from the second part of the nineteenth century to the
382 end of the twentieth century have left a huge environmental legacy, including several
383 acidic pit lakes that store high volumes of AMD (5.2 Mm^3 in July 2016), including
384 approximately 9,000 ton of dissolved Fe and 1,000 ton of dissolved Al and Zn.

385 Significant differences in the hydrological behavior of the flooded open pits have been
386 established. The water level in Filón Centro and Filón Sur seems to have reached a
387 stationary state, showing slight annual variations. The water balance in Filón Centro
388 provides evidence that this pit lake behaves as a terminal lake during dry and normal
389 periods, while during rainy periods it works as a flow-through pit lake, releasing water
390 through waste dumps located to the west of the lake. Filón Sur receives surface water
391 inputs that are much higher than losses by evaporation; thus, hidden losses may occur in
392 this pit lake through a derelict gallery to the east. Significant releases of acidic waters
393 must take place from this pit lake to the receiving water bodies.

394 The water level in Filón Norte and Sierra Bullones is rising an average of 2.8 m/yr after
395 the cease of mining at the end of the last century. The flooding of both pit lakes follows
396 a similar evolution because underground galleries connect them. Sierra Bullones
397 receives high inputs by runoff. Inputs are much higher than losses by evaporation and
398 the increments of water stored in the pit lake, which is evidence of the existence of
399 underground exits to Filón Norte. Water inputs by runoff and direct precipitation in

Filón Norte were higher than losses by evaporation. However, this situation has reversed since 2011 due to the increase in evaporation linked to the increment of flooded surface. In addition, the water balance provides evidence that losses from Sierra Bullones are quite similar to water inputs to Filón Norte up to 2009. However, water inputs to Filón Norte exceed the exits from Sierra Bullones in recent years, which indicate the existence of underground inputs from the surrounding area.

According to the water level prediction obtained from a polynomial regression, the outflow level in Filón Norte and Sierra Bullones would be reached by 2051. However, a simple approach based on the assumption that groundwater inputs remain constant would indicate that losses by evaporation would offset inputs (that is, runoff, direct precipitation, and groundwater inputs) before reaching the water outflow level. Nevertheless, a mathematical model based on high-resolution hydrogeological parameters of the area and a monitoring plan should be implemented in the future.

The information obtained in this study will allow for more cost-effective measures to be adopted mitigating the severe pollution by AMD, which affects the watercourses of this area. In addition, the methodology applied in this work could be of great interest for decision makers in other areas affected by opencast mining.

Acknowledgements

This work was supported by the Spanish Ministry of Economic and Competitiveness through the projects CGL2016-78783-C2-1-R (SCYRE) and ERAMIN PCIN2015-242. C.R. Cánovas was funded by the Talent consolidation program of the University of Huelva.

Conflict of Interest Statement

Conflict of Interest – None

References

Allen, R.G., Pereira, L.S., Raes, D. y Smith, M. (1998). Crop evapotranspiration. Guidelines for computing crop water requirements. FAO Irrigation and drainage paper 56. Rome, Italy, 300 p.

Blodau, C., 2006. A review of acidity generation and consumption in acidic coal mine lakes and their watersheds. Sci Total Environ 369: 307–332.

Geller, W., Schultze, M., Kleinman, R., Wolkersdorfer, (eds.) (2013). Acidic pit lakes. The legacy of coal and metal surface mines. Springer. Verlag, Berlin-Heidelberg, 525 p.

Boehrer, B., Yusta, I., Magin, K., Sanchez-España, J. (2016). Quantifying, assessing and removing the extreme gas load from meromictic Guadiana pit lake, Southwest Spain. Sci Total Environ 563-564: 468-477.

Cánovas, C.R., Peiffer, S, Macías, F., Olías, M., Nieto, J.M. (2015): Geochemical processes in a highly acidic pit lake of the Iberian Pyrite Belt (SW Spain). Chem Geol 395: 144–153.

Cánovas CR, Olias M, Macias F, Torres E, San Miguel EG, Galván L, Ayora C, Nieto JM (2016) Water acidification trends in a reservoir of the Iberian Pyrite Belt (SW Spain). Sci Total Environ 541: 400-41116)

445 Castendyk, D.N (2011). Lessons learned from pit lake planning and development. In:
446 Mine Pit Lakes: Closure and Management (Ed. C.D. McCullought). Australian Centre
447 for Geomechanics, University of Western Australia, 15-28.

448 Castendyk, D.N., Balistrieri, L.S., Gammons, C., Tucci, N. (2015a). Modeling and
449 management of pit lake water chemistry 2. Case Studies. Appl Geochem 57: 289-307.

450 Castendyk, D.N., Eary, L.E., Balistrieri, L.S. (2015b). Modeling and management of
451 pit lake water chemistry 1. Theory. Appl Geochem 57: 267-288.

452 Checkland, S.G. (1967): The mines of Tharsis. Roman, French and British entreprise in
453 Spain. Ed. George Allen & Unwin Ltd. London, 288 p.

454 Davis, A., Ashemberg, D. (1989): The aqueous geochemistry of the Berkeley pit, Butte,
455 Montana, USA. Appl Geochem 4: 23-36.

456 Deligny, E. (1863): Notas históricas sobre las minas de cobre de Sierra de Tharsis.
457 Revista Minera vol XIV, 111-121.

458 Galván, L., Olías, M., Fernandez de Villarán, R., Domingo Santos, J.M., Nieto, J.M.,
459 Sarmiento, A.M., Cánovas, C.R. (2009): Application of the SWAT model to an AMD-
460 affected river (Meca River, SW Spain). Estimation of transported pollutant load. J
461 Hydrol 377:445–454.

462 Gonzalo y Tarín, J. (1888): Descripción física, geológica y minera de la provincia de
463 Huelva. Memorias de la Comisión del Mapa Geológico de España, Tomo II. Madrid.
464 660 p.

465 Kirby, C.S., Cravotta III, C.A., (2005). Net alkalinity and net acidity 1: Theoretical
466 considerations. Appl. Geochem. 20 (10), 1920–1940.

Marinelli, F., Niccoli, W.N. (2000). Simple analytical equations for estimating groundwater inflow to a mine pit. Groundwater 38: 311-314.

Nordstrom, D.K., Blowes, D.W., Ptacek, C.J. (2015). Hydrogeochemistry and microbiology of mine drainage: An update. Appl Geochem 57: 3-16.

Oldham, C.E., Salmon, S.U., Hipsey, M.R., Ivey, G.N. (2009). Modeling pit lake water quality: Coupling of lake stratification dynamics, lake ecology, aqueous geochemistry, and sediment diagenesis. In: Mine pit lakes. Characteristics, predictive modeling and sustainability (Eds: Castendyk, N., Eary, L.E.). Society of Mining, Metallurgy & Exploration, Littletown, Colorado, 127-136.

Olías, M., Macías, F., Cánovas, C.R., Moreno, R. (2017): Características de algunas surgencias ácidas en acuíferos generados por la minería de sulfuros (SO ESPAÑA). Congress on Groundwater and Global Change in the Western Mediterranean, Granada, España, 37-42.

Olías, M., Nieto, J.M., Sarmiento, A.M., Cánovas, C.R., Galván, L. (2011). Water Quality in the Future Alcolea Reservoir (Odiel River, SW Spain): A Clear Example of the Inappropriate Management of Water Resources in Spain. Water Resour Manage 25: 201–215.

Olías, M., Nieto, J.M., Pérez-López, R., Cánovas, C.R., Macías, F., Sarmiento, A.M., Galván, L. (2016). Controls on acid mine water composition from the Iberian Pyrite Belt (SW Spain). Catena 137: 12-23.

Penman, H.L. (1948). Natural evaporation from open water, bare soil and grass. Proc. Roy. Soc. London, A193, 120-146.

489 Pinedo Vara, I. (1963): Piritas de Huelva. Su historia, minería y aprovechamiento.
490 Summa, Madrid.

491 Sánchez España, J., López Pamo, E., Santofimia, E., Aduvire, O., Reyes, J., Barettino,
492 D. (2005). Acid mine drainage in the Iberian Pyrite Belt (Odiel river watershed, Huelva,
493 SW Spain): Geochemistry, mineralogy and environmental implications. Appl.
494 Geochem. 20: 1320-1356

495 Sánchez-España, J., López-Pamo, E., Santofimia, E., Diez, M. (2008). The acidic mine
496 pit lakes of the Iberian Pyrite Belt: An approach to their physical limnology and
497 hydrogeochemistry. Appl. Geochem. 23: 1260-1287.

498 Sánchez-España, J., Diez-Ercilla, M., Pérez Cerdán, F., Yusta, I. Boyce, A.J. (2014).
499 Hydrological investigation of a multi-stratified pit lake using radioactive and stable
500 isotopes combined with hydrometric monitoring. J Hydrol 511: 494-508

501 Santofimia, E., López-Pamo, E. (2013). The role of surface water and mine groundwater
502 in the chemical stratification of an acidic pit lake (Iberian Pyrite Belt, Spain). J Hydrol
503 490: 21-31.

504 Savage, K.S., Bird, D.K., Ashley, R.P. (2000). Legacy of the California Gold Rush:
505 Environmental geochemistry of arsenic in the southern Mother Lode Gold District. Int
506 Geol Rev 42: 385-405.

507 Robles-Arena, V.M., Candela, L. (2010): Hydrological conceptual model
508 characterisation of an abandoned mine site in semiarid climate. The Sierra de
509 Cartagena-La Unión (SE Spain). Geologica Acta 8: 235-248.

510 Tornos, F., Gonzalez Clavijo, E., Spiro, B. (1997): The Filón Norte orebody, Tharsis,
511 Iberian Pyrite Belt: a proximal low-temperature shale-hosted massive sulphide in a thin-
512 skinned tectonic belt. Mineralium Deposita 33, 150–169.

513 Tornos, F., Lopez-Pamo, E., Sánchez-España, F.J. (2009): TheIberianPyriteBelt. In:
514 Spanish Geological Framework and Geosites (Eds: Agueda, J., Palacios, J. and
515 Salvador, C.I.). IGME, Madrid, p: 56-64.

516 Vandenberg, J.A, Lauzon, N., Prakash, S., Salzsauler, K (2011). Use of water quality
517 models for design and evaluation of pit lakes. In: Mine Pit Lakes: Closure and
518 Management (Ed. C.D. McCullought). Australian Centre for Geomechanics, University
519 of Western Australia, 63-80.

520 Younger, P.L, Banwart, S.A., Hedin, R.S. (2002). Mine water. Hydrology, Pollution,
521 Remediation.Kluwer Academic Publishers, London, 422 p.

522

523

524 TABLE CAPTIONS

525 Table 1. Main characteristics of the flooded open pits.

526 Table 2. Results from the hydrogeochemical analysis and estimation of the acidity and
527 amount of pollutants stored in the pit lakes (for Sierra Bullones, the concentrations of
528 Filón Norte are used). [1]Data from Galván et al. (2012).

529 Table 3. Evolution of the pit lakes and water balances (in thousands of m^3, except
530 flooded surface area, which is reported in hm^2, and water level, which is reported in m).

531

532 FIGURE CAPTIONS

533 Figure 1. Location map of the Tharsis mine complex showing the location of profiles
534 represented in Figures 5, 6, and 7.

535 Figure 2. Annual evolution of precipitation and evaporation in the study area.

536 Figure 3. Selected orthophotographs of Filón Norte and Sierra Bullones open pits from
537 1998 to 2016.

538 Figure 4. Evolution of A) water level and B) stored water in Filón Norte and Sierra
539 Bullones pit lakes.

540 Figure 5. Schematic hydrologic profile of Filón Centro in A) dry and normal and B) wet
541 years. The thickness of the arrows is proportional to the water flux. The profile location
542 is in Fig. 1.

543 Figure 6. Schematic hydrologic profile of Filón Sur. The thickness of the arrows is
544 proportional to the water flux. The profile location is in Fig. 1.

545 Figure 7. Schematic hydrologic profile of Sierra Bullones and Filón Norte. Water levels
546 from July 2016 are indicated. The thickness of the arrows is proportional to the water
547 flux. The profile location is in Fig. 1.

548 Figure 8. Evolution of hidden water losses from Sierra Bullones and hidden inputs to
549 Filón Norte.

550

Figure 1

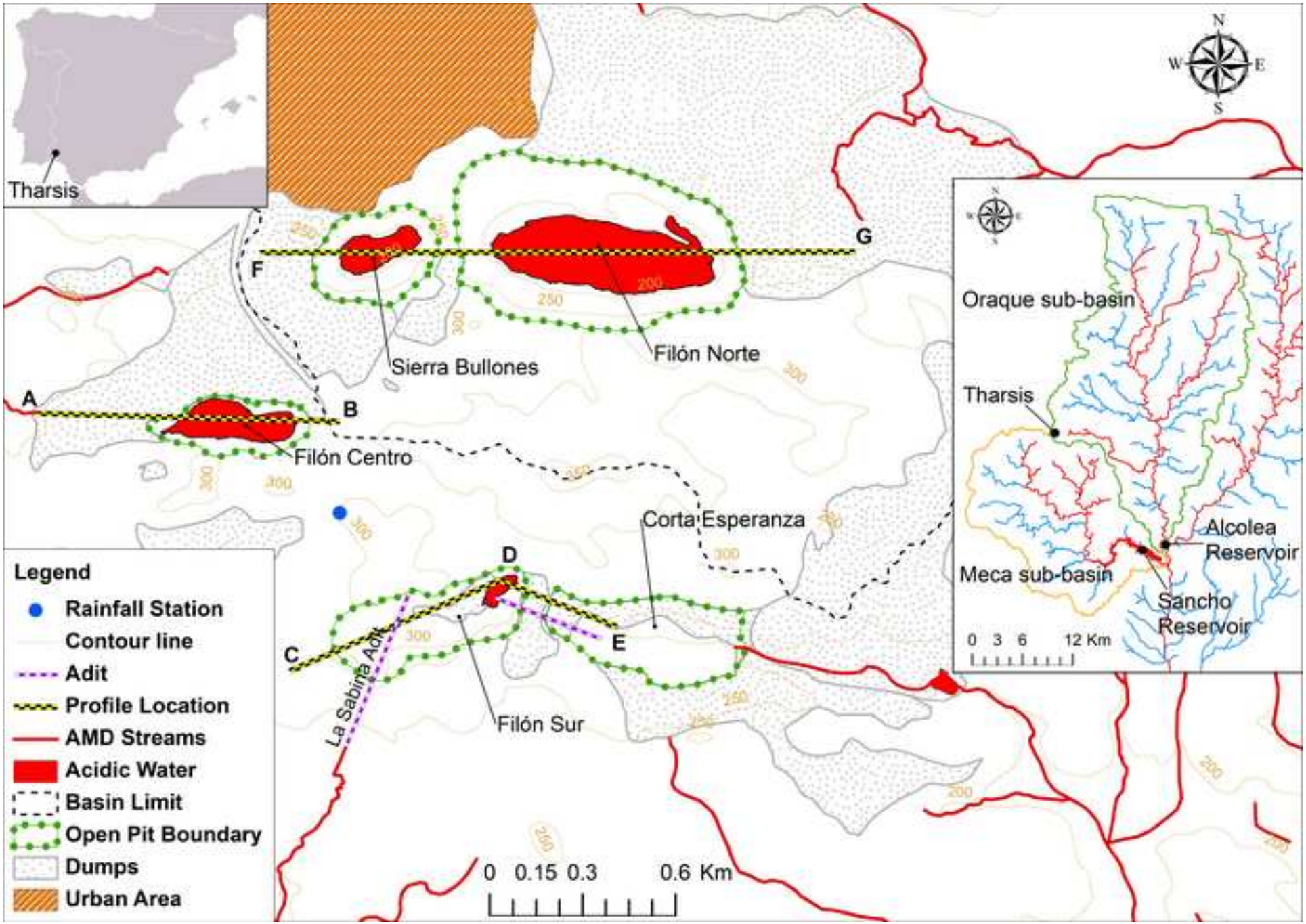
Tharsis
N
W
E
S
F
G
Sierra Bullones
Filón Norte
A
B
Filón Centro
Corta Esperanza
D
C
E
La Sabina Adit
Filón Sur
Legend
Rainfall Station
Contour line
Adit
Profile Location
AMD Streams
Acidic Water
Basin Limit
Open Pit Boundary
Dumps
Urban Area
0 0.15 0.3 0.6 Km
Oraque sub-basin
Tharsis
Alcolea Reservoir
Meca sub-basin
Sancho Reservoir
0 3 6 12 Km

Figure 2

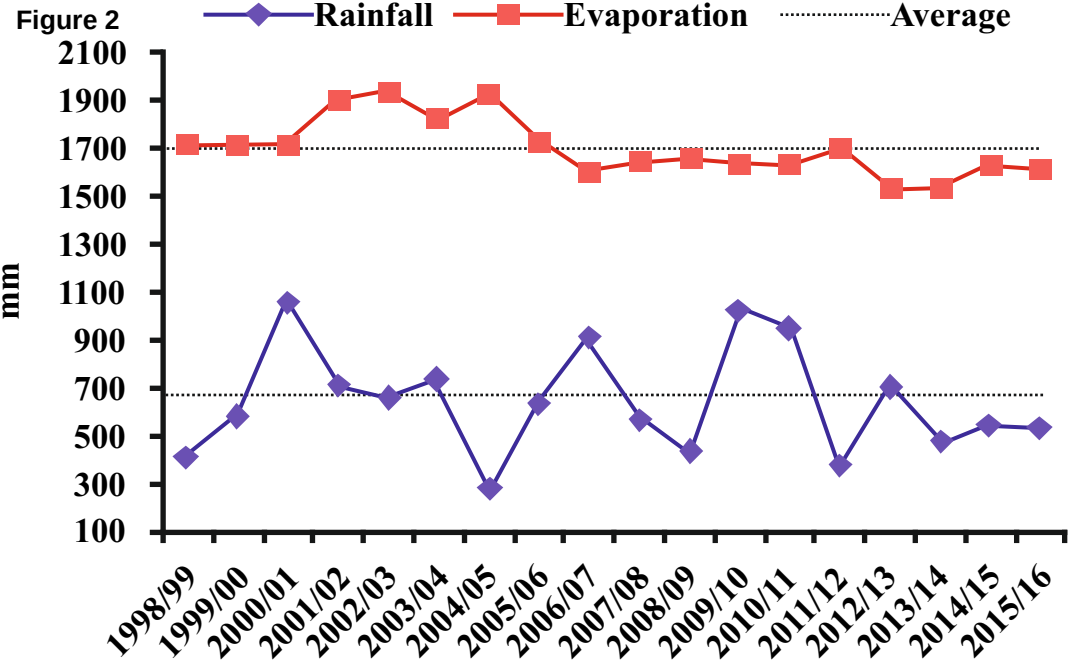
Rainfall
Evaporation
Average
mm
2100
1900
1700
1500
1300
1100
900
700
500
300
100
1998/99
1999/00
2000/01
2001/02
2002/03
2003/04
2004/05
2005/06
2006/07
2007/08
2008/09
2009/10
2010/11
2011/12
2012/13
2013/14
2014/15
2015/16

Figure 3

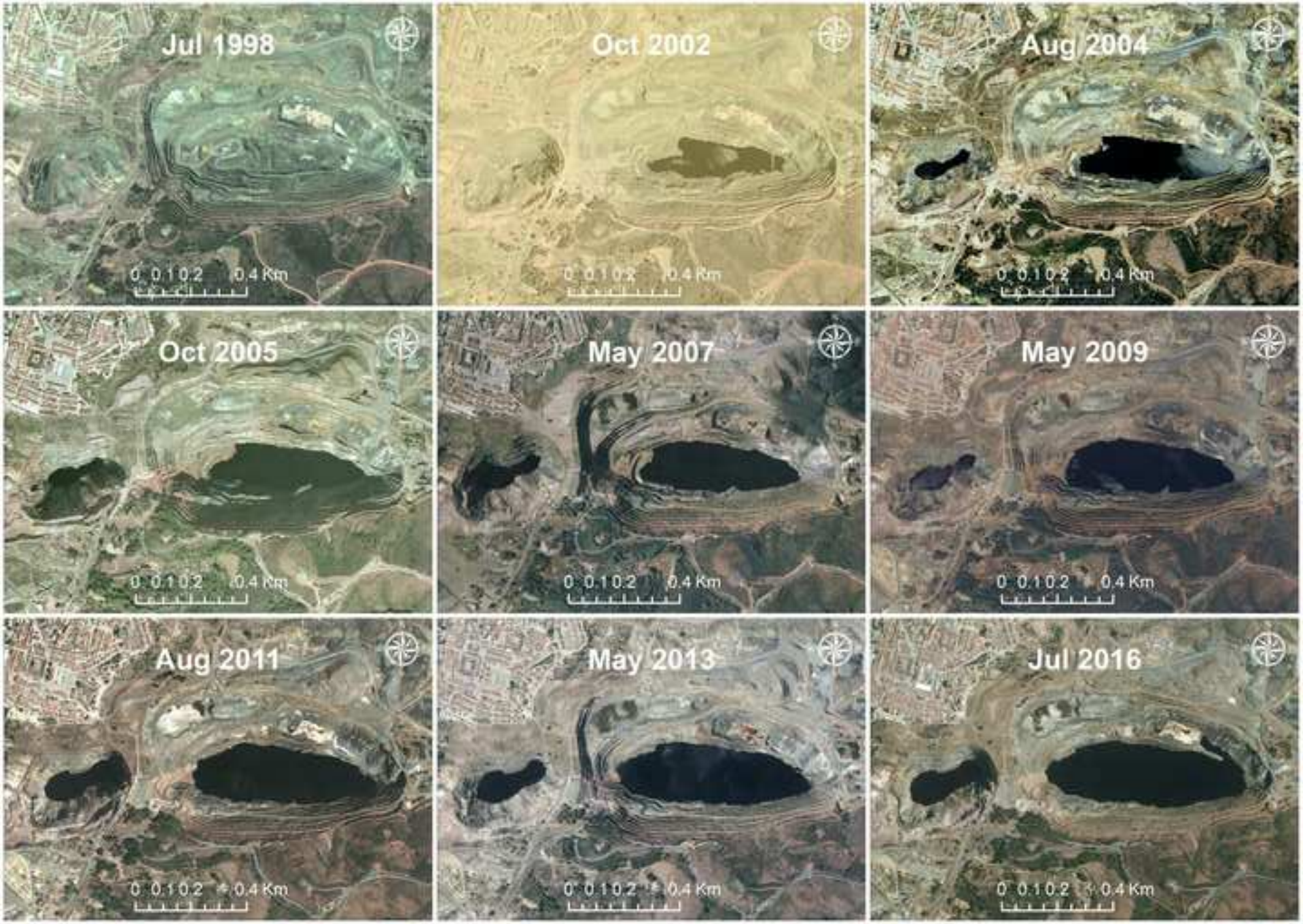
Jul 1998
Oct 2002
Aug 2004
Oct 2005
May 2007
May 2009
Aug 2011
May 2013
Jul 2016
0 0.1 0.2 0.4 Km

Figure 4

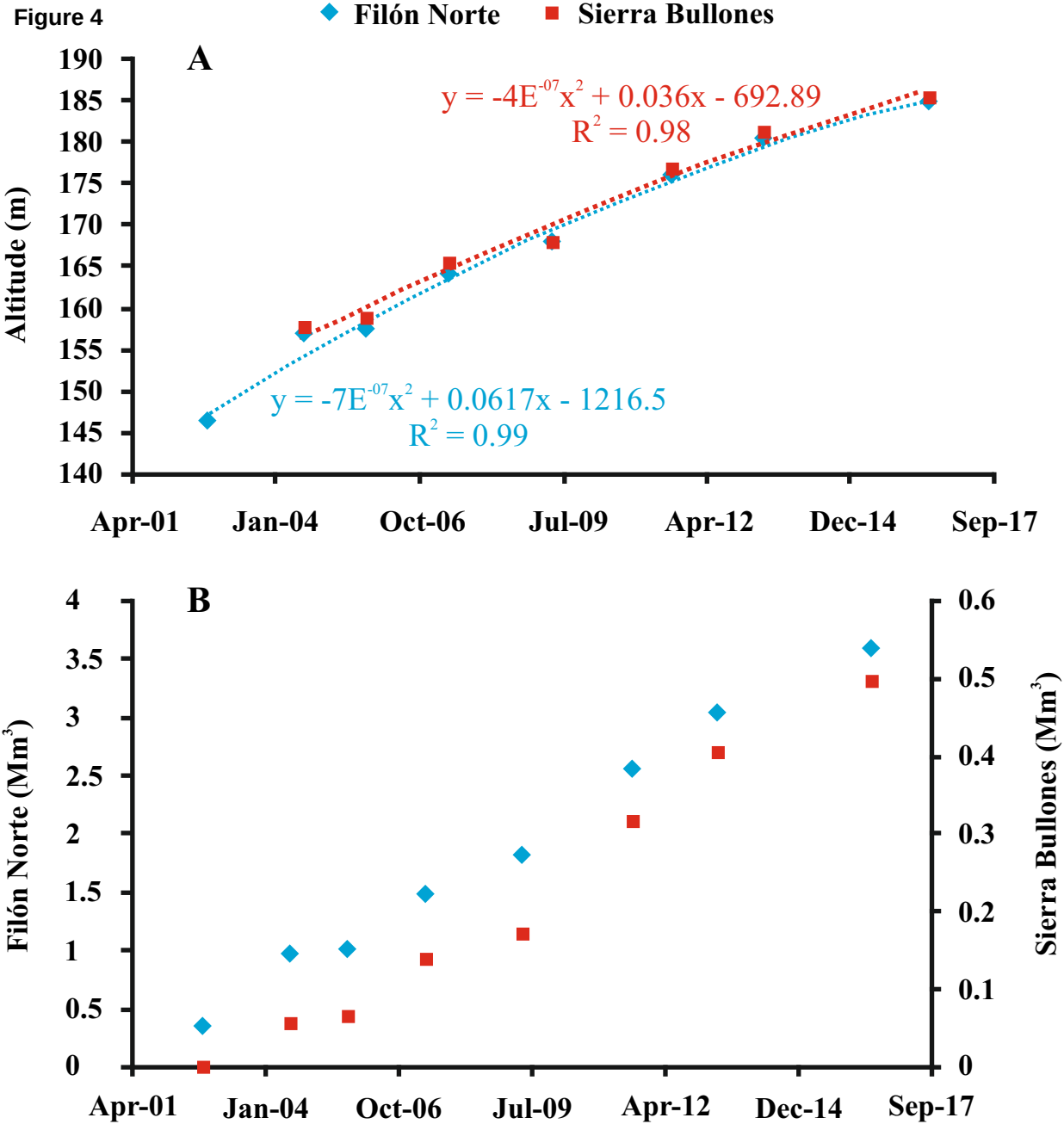
Filón Norte
Sierra Bullones
A
y = -4E-07x2 + 0.036x - 692.89
R2 = 0.98
y = -7E-07x2 + 0.0617x - 1216.5
R2 = 0.99
Altitude (m)
190
185
180
175
170
165
160
155
150
145
140
Apr-01
Jan-04
Oct-06
Jul-09
Apr-12
Dec-14
Sep-17
B
Filón Norte (Mm3)
Sierra Bullones (Mm3)
4
3.5
3
2.5
2
1.5
1
0.5
0
0.6
0.5
0.4
0.3
0.2
0.1
0
Apr-01
Jan-04
Oct-06
Jul-09
Apr-12
Dec-14
Sep-17

Figure 5

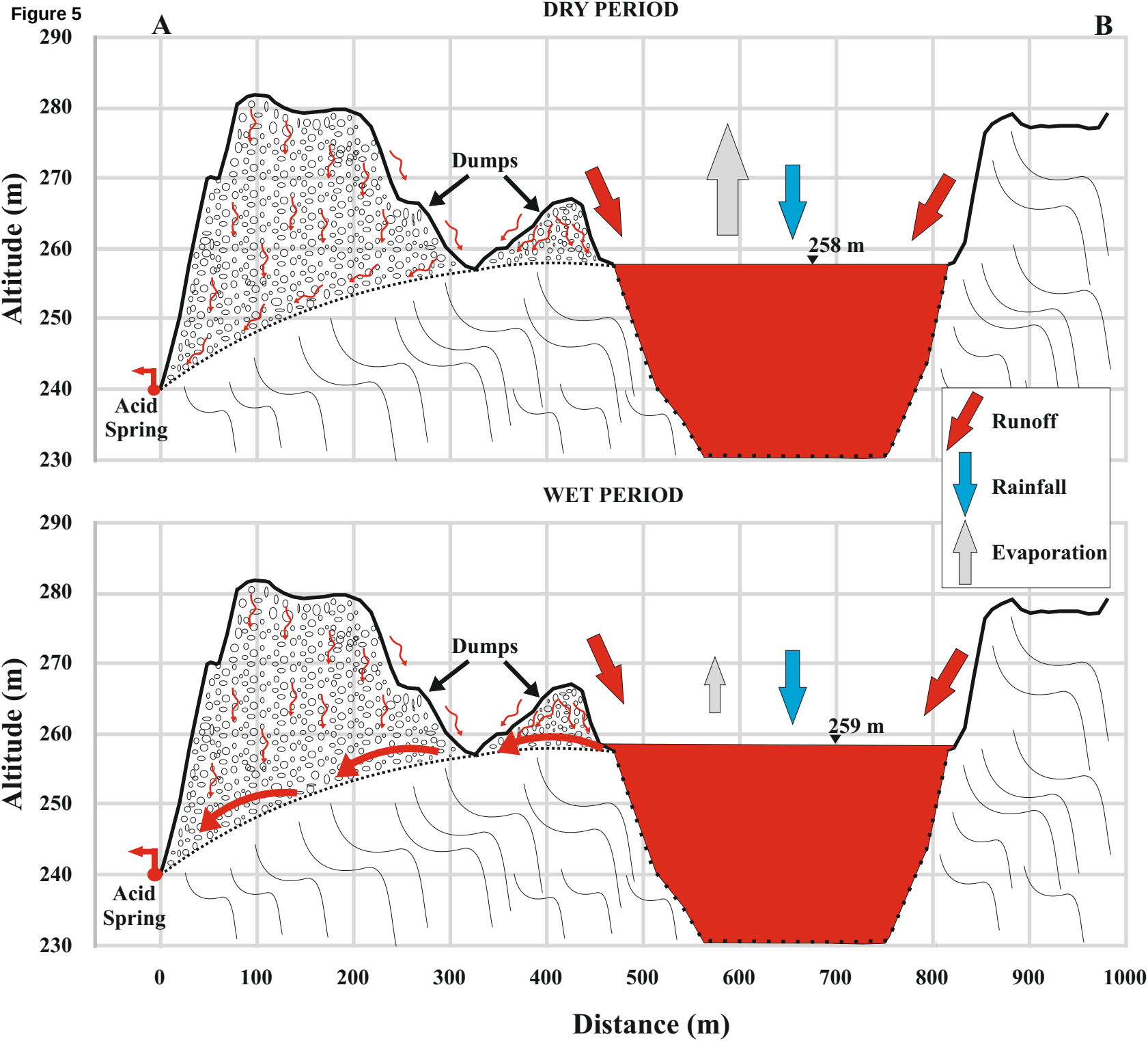
A
DRY PERIOD
B
Altitude (m)
290
280
270
260
250
240
230
Dumps
258 m
Acid
Spring
Runoff
Rainfall
Evaporation
WET PERIOD
Dumps
259 m
Acid
Spring
0
100
200
300
400
500
600
700
800
900
1000
Distance (m)

Figure 6

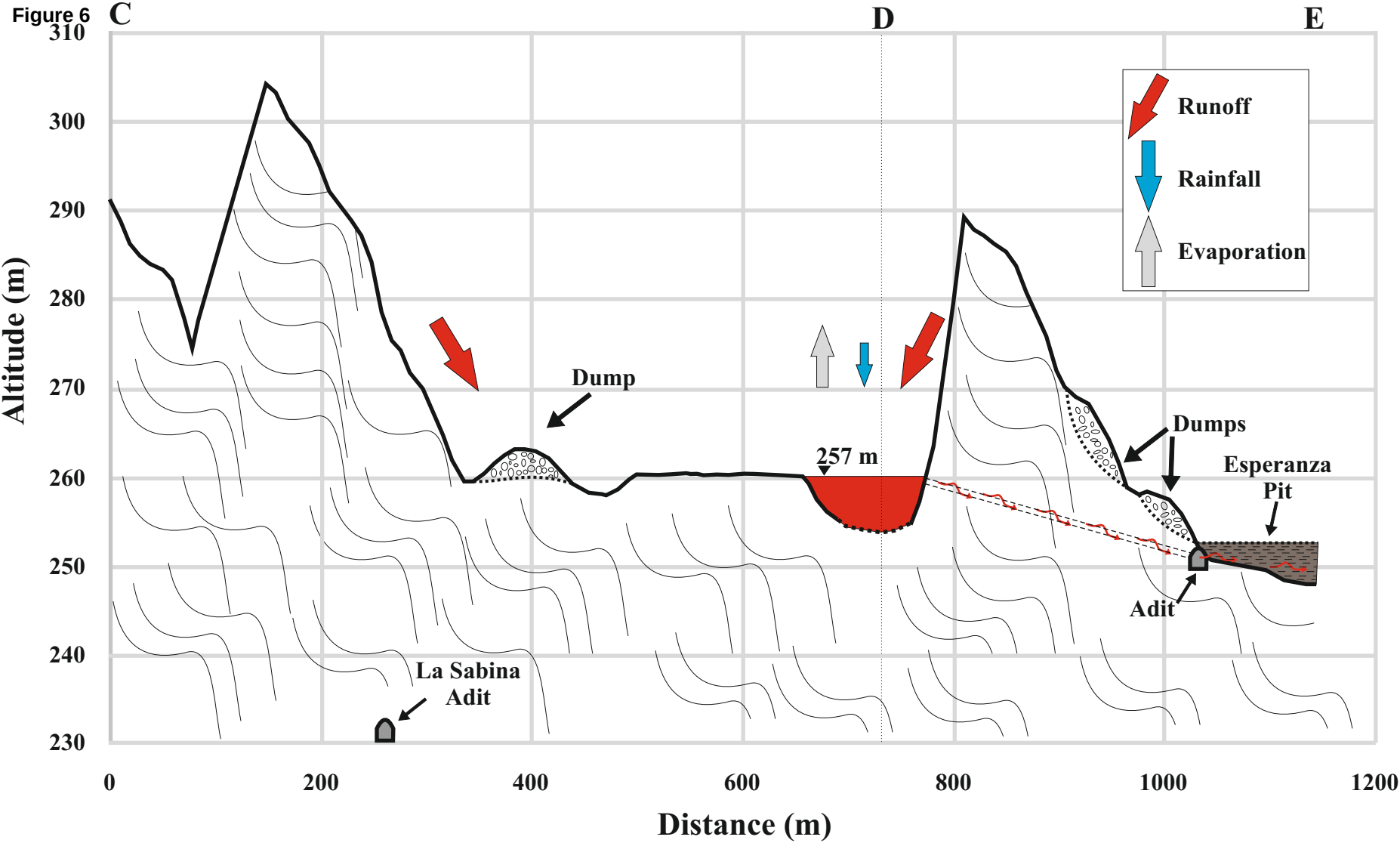
C
D
E
Runoff
Rainfall
Evaporation
Dump
257 m
Dumps
Esperanza
Pit
Adit
La Sabina
Adit
Altitude (m)
310
300
290
280
270
260
250
240
230
0
200
400
600
800
1000
1200
Distance (m)

Figure 7

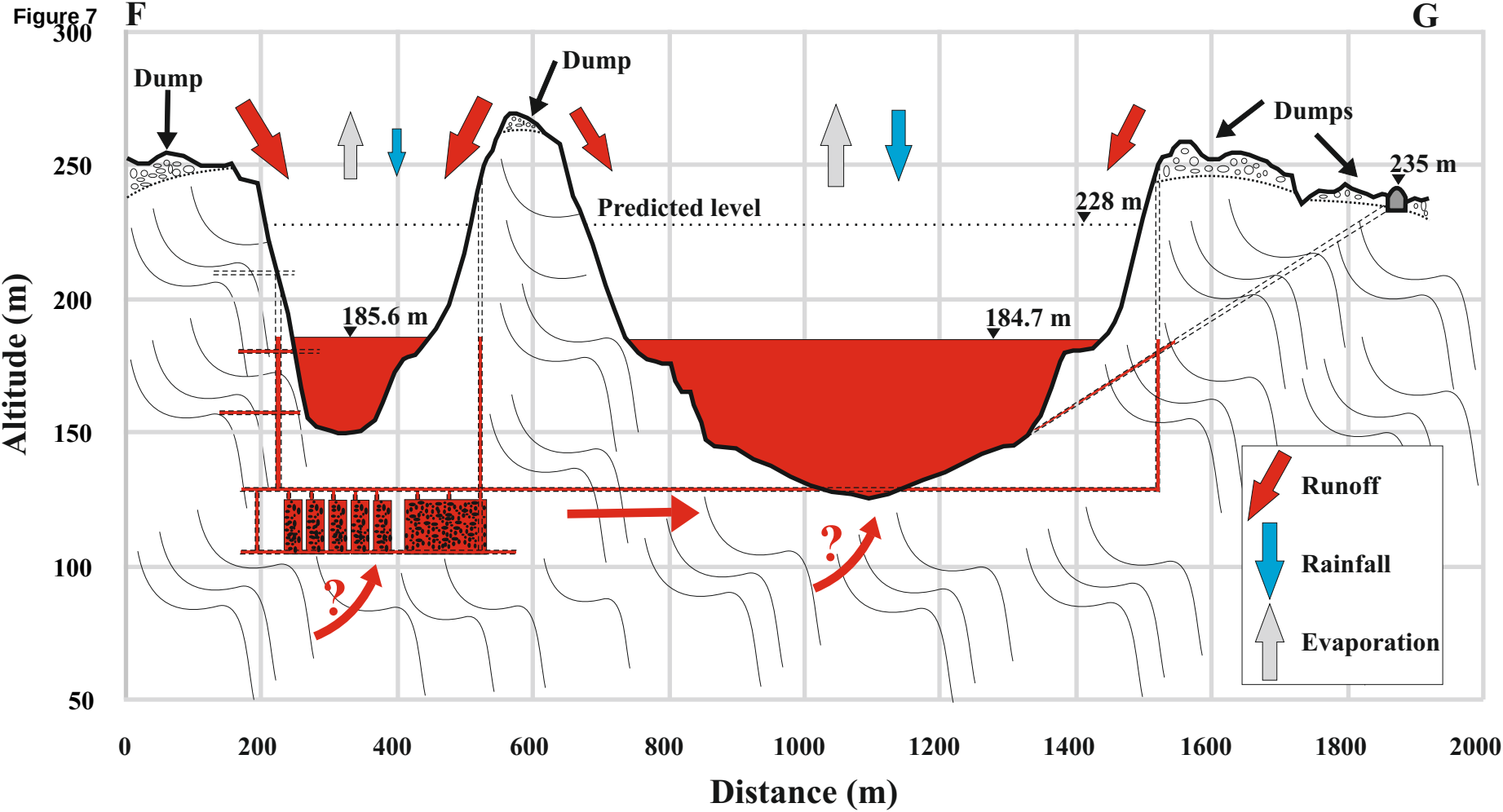
F
G
Dump
Dump
Dumps
235 m
Predicted level
228 m
185.6 m
184.7 m
?
?
Runoff
Rainfall
Evaporation
Altitude (m)
300
250
200
150
100
50
0
200
400
600
800
1000
1200
1400
1600
1800
2000
Distance (m)

Figure 8

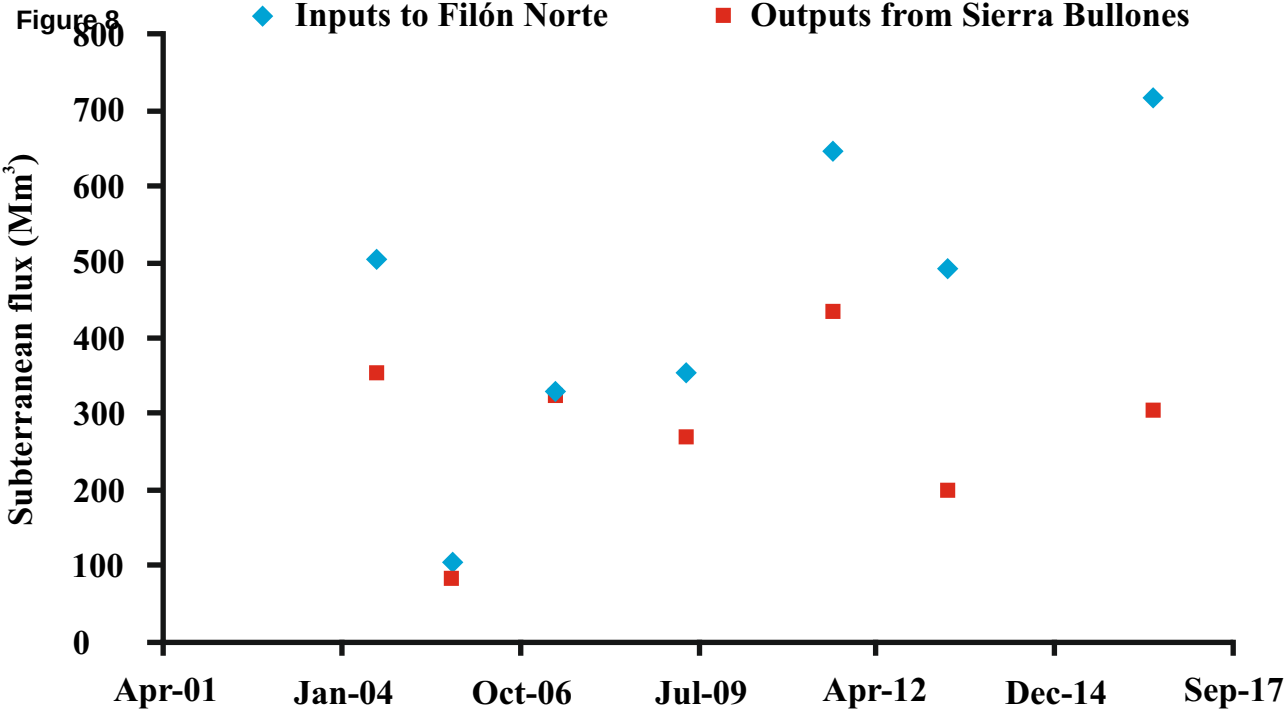
Inputs to Filón Norte
Outputs from Sierra Bullones
Subterranean flux (Mm3)
800
700
600
500
400
300
200
100
0
Apr-01
Jan-04
Oct-06
Jul-09
Apr-12
Dec-14
Sep-17

Table 1

	Drainage basin (hm^2)	Pit surface (hm^2)	Lengh (m)	Width (m)	Depth (m)	End of mining
Filón Norte	60	52	914	541	126	1999
Filón Sur	29	13	657	430	22	2001
Sierra Bullones	104	10	426	300	102	1966
Filón Centro	20	7	527	194	46	1960

Table 2

Pit lake	pH	EC mS/cm	Acidity g/L $CaCO_3$	Al mg/L	Cu mg/L	Fe mg/L	Mn mg/L	Sulfate mg/L	Zn mg/L	As µg/L	Cd µg/L	Co µg/L	Cr µg/L
Filón Sur	2.23	3.07	3.6	223	53	774	5.3	3951	10	1461	67	3751	138
Filón Norte	2.25	4.84	7.1	217	41	2053	40	8529	228	11360	648	4821	216
Filón Centro	2.32	2.93	2.6	138	12	569	26	4038	25	209	67	1314	32

	Stored water (Mm^3)	Stored amount (ton)										
Filón Sur	0.0058	21	1.3	0.3	4.5	0.03	23	0.06	0.008	0.000	0.022	0.001
Filón Norte	3.58	25271	777	147	7350	143	30534	816	40.7	2.32	17.3	0.77
Sierra Bullones	0.50	3530	109	21	1027	20	4265	114	5.68	0.32	2.41	0.11
Filón Centro	1.10	2860	152	13	626	29	4442	28	0.23	0.07	1.45	0.04
Total	5.19	31682	1038	181	9007	192	39263	958	46.6	2.72	21.1	0.92

	Load (ton/year)										
Average Meca River load[1]	3183	595	74	255	90	9174	181	0.06	0.36	5.4	0.15

Table 3

	Period	Flooded surface (hm^2)	Water level (m)	Water volume (Mm^3)	Surface Inputs (I_n) (Mm^3)		Evapor. (O_n) (Mm^3)	I_n-O_n (Mm^3)
					Runoff ($Qrun_n$)	Rainfall (DR_n)		
Filón Centro	Jul 98 - Oct 02	3.6	258.6	1.022	0.137	0.104	0.285	-0.044
	Nov 02 - Aug 04	3.6	258.6	1.038	0.065	0.050	0.128	-0.014
	Sep 04 - Oct 05	3.4	258.2	0.980	0.017	0.013	0.077	-0.048
	Nov 05 - May 07	3.7	258.7	1.051	0.064	0.050	0.087	0.026
	Jun 07- May 09	3.7	258.6	1.047	0.052	0.040	0.123	-0.031
	Jun 09 - Aug 11	3.6	258.5	1.028	0.095	0.073	0.146	0.022
	Sep 11 - May 13	3.7	258.7	1.051	0.050	0.039	0.096	-0.007
	Jun 13 - Jul 16	3.8	258.7	1.059	0.077	0.060	0.181	-0.044
Filón Sur	Jul 98 - Oct 02	0.4	256.2	0.005	0.245	0.006	0.018	0.234
	Nov 02 - Aug 04	0.5	256.5	0.005	0.114	0.007	0.009	0.112
	Sep 04 - Oct 05	0.4	255.7	0.004	0.031	0.002	0.004	0.028
	Nov 05 - May 07	0.7	256.9	0.007	0.112	0.007	0.009	0.111
	Jun 07- May 09	0.5	256.4	0.005	0.091	0.007	0.008	0.089
	Jun 09 - Aug 11	0.8	257.0	0.008	0.168	0.013	0.016	0.165
	Sep 11 - May 13	0.7	257.0	0.007	0.088	0.008	0.009	0.087
	Jun 13 - Jul 16	0.6	256.7	0.006	0.135	0.010	0.013	0.132
Sierra Bullones	Jul 98 - Oct 02	0.0	-	0.000	0.893	0.000	0.000	0.893
	Nov 02 - Aug 04	0.9	157.6	0.055	0.419	0.006	0.016	0.409
	Sep 04 - Oct 05	0.9	158.7	0.065	0.111	0.003	0.021	0.093
	Nov 05 - May 07	1.3	165.5	0.139	0.410	0.015	0.026	0.399
	Jun 07- May 09	1.4	167.8	0.171	0.333	0.015	0.045	0.303
	Jun 09 - Aug 11	1.9	176.7	0.315	0.612	0.032	0.065	0.579
	Sep 11 - May 13	2.1	181.3	0.404	0.319	0.021	0.051	0.289
	Jun 13 - Jul 16	2.3	185.4	0.496	0.490	0.036	0.128	0.398
Filón Norte	Jul 98 - Oct 02	4.4	146.2	0.348	0.496	0.062	0.171	0.387
	Nov 02 - Aug 04	6.4	156.7	0.956	0.221	0.072	0.187	0.106
	Sep 04 - Oct 05	6.5	157.3	0.996	0.058	0.023	0.143	-0.062
	Nov 05 - May 07	7.7	163.9	1.464	0.211	0.094	0.166	0.139
	Jun 07- May 09	8.8	168.0	1.801	0.167	0.089	0.273	-0.017
	Jun 09 - Aug 11	10.3	175.9	2.556	0.302	0.190	0.380	0.112
	Sep 11 - May 13	11.4	180.3	3.034	0.154	0.112	0.277	-0.011
	Jun 13 - Jul 16	12.9	184.9	3.589	0.230	0.194	0.585	-0.160